The essential relationship between deadbeat predictive control and continuous-control-set model predictive control for PWM converters

Bi Liu[1], Tao Chen[2], and Wensheng Song[1*]

1. Department of Electrical Engineering, Southwest Jiaotong University, Chengdu, 610031, China
2. CRRC Zhuzhou Institute Co., Ltd, Zhuzhou 412001, China

*E-mail: songwsh@swjtu.edu.cn

***Abstract*-This paper presents the equivalent principle of deadbeat predictive direct power control (DP-DPC) scheme and conventional continuous-control-set model predictive direct power control (MP-DPC) scheme of single-phase pulse width modulation (PWM) ac-dc converters, respectively, and reveals their inherent relationship from the view of the expressions of modulated voltage vector in *dq* rotating frame. The expression of the modulation index can be derived from the expression of modulated voltage vector in conventional MP-DPC scheme, which is in accordance with the result in the MP-DPC scheme with modulation function optimization. On this basis, the relationship of these CCS MP-DPC schemes with the same cost function is discussed in this paper. A comprehensive experimental comparison has been conducted, experimental results confirm the theoretical study and the effectiveness of the three DPC schemes.**

***Keywords*-direct power control, model predictive control, continuous-control-set, single-phase PWM converter.**

I. INTRODUCTION

Due to the excellent characteristics, such as bidirectional energy flow, high power factor, low current harmonics and good dc-link voltage regulation, single-phase pulse width modulation (PWM) ac-dc converters have been widely used in railway locomotive traction [1]. Therefore various control schemes have been reported in recent decades. Direct power/current control is an alternative control solution for single-phase PWM converters, which can realize good steady-state and rapid dynamic performance. For the similar characteristics between direct current control and direct power control (DPC), DPC is taken as a case study in this paper.

For the classical DPC scheme choosing the relevant converter switching state through a look-up table for the hysteresis comparators, it has many excellent properties: simple system configuration, high executing efficiency and fast dynamic response [2]. However, a high sampling frequency is necessary in this DPC scheme, and the switching frequency is variable [3]. To overcome those drawbacks, variable DPC schemes have been proposed to stabilize switching frequency, such as PI-based DPC [4], deadbeat predictive DPC (DP-DPC) [5][6], and continuous-control-set model predictive DPC (MP-DPC) schemes with PWM stage or vector sequences with optimized duty cycle control [7][8]. Recently, DP-DPC and MP-DPC schemes become two well-known approaches in power converters application. In order to track the desired reference active and reactive powers, the DP-DPC with PWM scheme uses the system predictive model to calculate the desired modulation voltage vector during each sampling interval and adopts PWM stage to generate the gating signals [6]. And the conventional MP-DPC with PWM scheme defines a cost function as a criterion, selects the optimal modulation voltage vector while the minimization of the cost function is achieved [7]. Due to the accurate steady characteristic and fast dynamic response, much effort has been done on the advanced MP-DPC scheme. [8] presents a MP-DPC scheme with modulation function optimization, which applies the cost function to predict the optimal modulation index in two-axis stationary reference frame. The MP-DPC with duty cycle optimization is proposed in [9], which calculates the optimal duty cycle of the nonzero vector and a zero vector within a control interval.

However, there are few literatures for discussing the inherent relationship between DP-DPC and continuous-control-set MP-DPC with PWM stage. Thus, in this paper, the principles of the former two DPC schemes in single-phase PWM converters and the inherent relation between them are presented. The rest of this paper is organized as follows. Section II describes a power mathematical model of single-phase two-level PWM converters. The principle of DP-DPC and the conventional MP-DPC scheme is introduced in Section III, then the inherent relationship among the DP-DPC and continuous-control-set MP-DPC schemes, and the MP-DPC scheme with modulation function optimization scheme is revealed in Section IV. An experimental test of the conventional MP-DPC scheme is conducted in Section V, followed by a conclusion in Section VI.

II. SYSTEM DESCRIPTION AND MATHEMATICAL MODEL

Fig. 1 shows the topology of a single-phase two-level PWM converter, where u_s and i_s are the main voltage and the line current, respectively; u_{ab}, i_L and u_{dc} represent the input voltage of H-bridge, the dc-link current and dc-link voltage of the converter, respectively; L_s and R_s are symbols for the equivalent resistance and inductance of ac-side inductors; C_d

and R_L are the dc-link capacitor and equivalent resistive load; S_1, S_2, S_3 and S_4 represent IGBT modules with anti-parallel diodes on the converter's leg-a and leg-b, respectively.

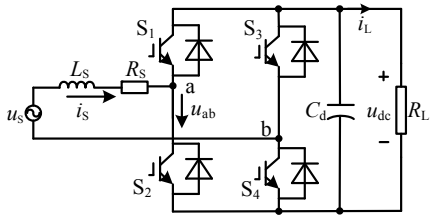

Fig. 1 The topology of a single phase two-level converter

As shown in Fig. 1, the mathematical model of the adopted converter can be expressed as

$$L_s \frac{di_s}{dt} = u_s - R_s i_s - u_{ab} \tag{1}$$

On the basis of three-phase instantaneous power theory, the instantaneous active power and reactive power of the adopted converter can be shown as [10]

$$\begin{bmatrix} P \\ Q \end{bmatrix} = \frac{1}{2}\begin{bmatrix} u_{s\alpha} & u_{s\beta} \\ u_{s\beta} & -u_{s\alpha} \end{bmatrix}\begin{bmatrix} i_{s\alpha} \\ i_{s\beta} \end{bmatrix} = \frac{1}{2}\begin{bmatrix} u_{sd} & u_{sq} \\ u_{sq} & -u_{sd} \end{bmatrix}\begin{bmatrix} i_{sd} \\ i_{sq} \end{bmatrix} \tag{2}$$

where P and Q are the instantaneous active and reactive powers, respectively. $u_{s\alpha}$, $u_{s\beta}$ represent the α-axis and β-axis components of the main voltage vector $\boldsymbol{u_s}$; $i_{s\alpha}$, $i_{s\beta}$ represent the α-axis and β-axis components of the line current vector $\boldsymbol{i_s}$ in $\alpha\beta$ stationary coordinate frame. u_{sd}, u_{sq} are the d-axis and q-axis components of $\boldsymbol{u_s}$; i_{sd}, i_{sq} are the d-axis and q-axis components of $\boldsymbol{i_s}$ in dq rotating frame.

According to (2), the fictitious β-axis components of $\boldsymbol{u_s}$ and $\boldsymbol{i_s}$ need to be generated to estimate the instantaneous active and reactive powers in single-phase converter system. Then the second-order generalized integral (SOGI) method is adopted to estimate the fictitious β-axis components of $\boldsymbol{u_s}$ and $\boldsymbol{i_s}$ in this paper, which can present advantages such as noise and harmonic filtering, simple structure, the adaptive characteristic and fast dynamic response [11].The transfer function expression of SOGI in s-domain can be written as

$$\begin{cases} x_\alpha(s) = \dfrac{k\omega s}{s^2 + k\omega s + \omega^2} x(s) \\ x_\beta(s) = \dfrac{k\omega^2}{s^2 + k\omega s + \omega^2} x(s) \end{cases} \tag{3}$$

where ω represents angular frequency of the main voltage u_s, k is the damping factor, and the outstanding performance of SOGI depends on the selection of damping factor k. [11] gives an optimal value of k to gain the fastest response while k=1.57.

Applying (3) to the main voltage u_s and the line current i_s, respectively, the block diagram of calculating $u_{s\alpha}$, $u_{s\beta}$, $i_{s\alpha}$, $i_{s\beta}$, P and Q is shown in Fig. 2.

The $\alpha\beta/dq$ transformation in Fig. 2, can be expressed as

$$\begin{bmatrix} d \\ q \end{bmatrix} = \begin{bmatrix} \cos\omega t & \sin\omega t \\ -\sin\omega t & \cos\omega t \end{bmatrix}\begin{bmatrix} \alpha \\ \beta \end{bmatrix} \tag{4}$$

From (1), the mathematical model in d-q frame of the adopted converters can be written as

$$\begin{cases} L_s \dfrac{di_{sd}}{dt} = u_{sd} - R_s i_{sd} - u_{abd} + \omega L_s i_{sq} \\ L_s \dfrac{di_{sq}}{dt} = u_{sq} - R_s i_{sq} - u_{abq} - \omega L_s i_{sd} \end{cases} \tag{5}$$

where u_{abd}, u_{abq} represent the d-axis and q-axis components of the modulated voltage vector $\boldsymbol{u_{ab}}$.

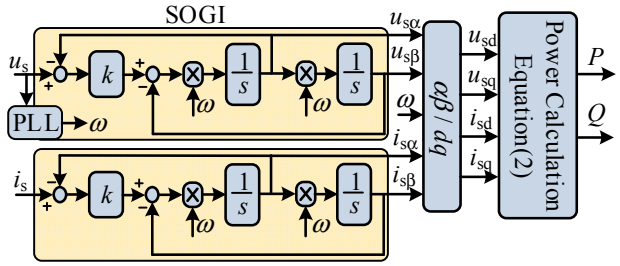

Fig. 2 Block diagram of instantaneous powers estimation of the adopted converter

Assuming that there is no fluctuation in the main voltage u_s, then the d-axis and q-axis voltage components u_{sd}, u_{sq} are constant values in normal condition. Generally, the main voltage u_s is orientated to d axis, in the d-q reference frame, where $u_{sd} = U_{sm}$, $u_{sq} = 0$. And U_{sm} is the peak values of the fundamental components in the main voltage u_s. Then substituting (2) into (5), the power mathematical model of single-phase PWM converter is shown as

$$\begin{cases} L_s \dfrac{dP}{dt} = \dfrac{1}{2}U_{sm}^2 - \dfrac{1}{2}u_{abd}U_{sm} - R_s P - \omega L_s Q \\ L_s \dfrac{dQ}{dt} = \dfrac{1}{2}u_{abq}U_{sm} - R_s Q + \omega L_s P \end{cases} \tag{6}$$

III. Conventional DP-DPC and MP-DPC of the Adopted Converter

A. Principle of DP-DPC scheme

The equivalent resistance R_s is very small and can be ignored. Then, applying the first-order discrete approximation to the power mathematical model expressed in (6), the (k+1)th power sampling values are expressed as

$$\begin{cases} P(k+1) = P(k) + \dfrac{T_s}{L_s}\left(\dfrac{1}{2}U_{sm}^2(k) - \dfrac{1}{2}u_{abd}(k)U_{sm}(k) - \omega L_s Q(k)\right) \\ Q(k+1) = Q(k) + \dfrac{T_s}{L_s}\left(\dfrac{1}{2}u_{abq}(k)U_{sm}(k) + \omega L_s P(k)\right) \end{cases} \tag{7}$$

where T_s is the sampling interval.

In order to eliminate the power errors at the (k+1)th sampling interval successfully, in DP-DPC $P(k+1)$ and $Q(k+1)$ can be expressed as

$$\begin{cases} P(k+1) = P^* \\ Q(k+1) = Q^* \end{cases} \tag{8}$$

By replacing (8) into (7), the reference values of the modulation voltages that satisfy the control law in (8) are obtained as

$$\begin{cases} u_{\mathrm{abd}}(k) = U_{\mathrm{sm}}(k) - \dfrac{2L_{\mathrm{s}}}{U_{\mathrm{sm}}(k)T_{\mathrm{s}}}\left[P^{*} - P(k)\right] - \dfrac{2\omega L_{\mathrm{s}} Q(k)}{U_{\mathrm{sm}}(k)} \\ u_{\mathrm{abq}}(k) = \dfrac{2L_{\mathrm{s}}}{U_{\mathrm{sm}}(k)T_{\mathrm{s}}}\left[Q^{*} - Q(k)\right] - \dfrac{2\omega L_{\mathrm{s}} P(k)}{U_{\mathrm{sm}}(k)} \end{cases} \tag{9}$$

Then, transforming the reference voltages calculated from (9) to the α-β reference frame, which can be expressed as

$$\begin{bmatrix} u_{\mathrm{ab}\alpha}(k) \\ u_{\mathrm{ab}\beta}(k) \end{bmatrix} = \begin{bmatrix} \cos\omega t & -\sin\omega t \\ \sin\omega t & \cos\omega t \end{bmatrix} \begin{bmatrix} u_{\mathrm{abd}}(k) \\ u_{\mathrm{abq}}(k) \end{bmatrix} \tag{10}$$

where $u_{\mathrm{ab}\alpha}$, $u_{\mathrm{ab}\beta}$ represent the α-axis and β-axis components of the modulated voltage vector $\boldsymbol{u}_{\mathbf{ab}}$ in two-phase stationary coordinate system. The fictitious signal $u_{\mathrm{ab}\beta}$ is discarded and $u_{\mathrm{ab}\alpha}$ will be accepted as the reference value for the PWM generator. The modulated voltage $u_{\mathrm{ab}\alpha}$ is limited by dc-link voltage of the adopted converter, and the amplitude of $|u_{\mathrm{ab}\alpha}|$ is lower than u_{dc} in normal condition. If the $|u_{\mathrm{ab}\alpha}(k)|$ is larger than u_{dc}, the optimized $u_{\mathrm{abd}}(k)$ and $u_{\mathrm{abq}}(k)$ are out of the linear operation range. In this condition, the modulated voltage $u_{\mathrm{ab}\alpha}$ remains u_{dc} or $-u_{\mathrm{dc}}$, which can be expresses as

$$u_{\mathrm{ab}\alpha} = \mathrm{sgn}\left(u_{\mathrm{ab}\alpha}(k)\right) u_{\mathrm{dc}} \tag{11}$$

where $\mathrm{sgn}(u_{\mathrm{ab}\alpha}(k))$ represents the polarity of $u_{\mathrm{ab}\alpha}(k)$. Fig. 3 shows the control block of the DP-DPC scheme.

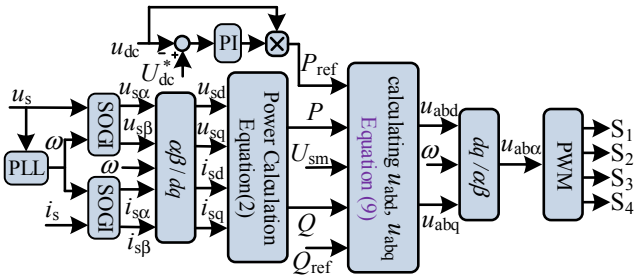

Fig. 3 Block diagram of the DP-DPC scheme

B. Principle of MP-DPC scheme

The control goal of MP-DPC is that the active and reactive powers are forced to track their references, respectively. Therefore, the cost function is usually defined as

$$J(k) = \left[P^{*} - P(k+1)\right]^{2} + \lambda\left[Q^{*} - Q(k+1)\right]^{2} \tag{12}$$

where λ represents the weighting factor of cost function. Substituting $P(k+1)$ and $Q(k+1)$ of (7) into (12), the cost function can be rewritten as

$$\begin{aligned} J(k) = {} & \left(\frac{U_{\mathrm{sm}}(k)T_{\mathrm{s}}}{2L_{\mathrm{s}}}\right)^{2} \left[u_{\mathrm{abd}}(k) - \left(U_{\mathrm{sm}}(k) - \frac{2\omega L_{\mathrm{s}} Q(k)}{U_{\mathrm{sm}}(k)} - \frac{2L_{\mathrm{s}}}{U_{\mathrm{sm}}(k)T_{\mathrm{s}}}\left(P^{*} - P(k)\right)\right)\right]^{2} \\ & + \lambda\left(\frac{U_{\mathrm{sm}}(k)T_{\mathrm{s}}}{2L_{\mathrm{s}}}\right)^{2} \left[u_{\mathrm{abq}}(k) - \left(-\frac{2\omega L_{\mathrm{s}} P(k)}{U_{\mathrm{sm}}(k)} + \frac{2L_{\mathrm{s}}}{U_{\mathrm{sm}}(k)T_{\mathrm{s}}}\left(Q^{*} - Q(k)\right)\right)\right]^{2} \end{aligned} \tag{13}$$

The optimization control object is to minimize the cost function $J(k)$ in (13) by calculating appropriate control variables $u_{\mathrm{abd}}(k)$ and $u_{\mathrm{abq}}(k)$, which yields

$$\begin{cases} \dfrac{\partial J(k)}{\partial u_{\mathrm{abd}}(k)} = 0 \\ \dfrac{\partial J(k)}{\partial u_{\mathrm{abq}}(k)} = 0 \end{cases} \tag{14}$$

Solving the simultaneous (13) and (14), the optimized voltage variables $u_{\mathrm{abd}}(k)$ and $u_{\mathrm{abq}}(k)$ can be derived as

$$\begin{cases} u_{\mathrm{abd}}(k) = U_{\mathrm{sm}}(k) - \dfrac{2L_{\mathrm{s}}}{U_{\mathrm{sm}}(k)T_{\mathrm{s}}}\left[P^{*} - P(k)\right] - \dfrac{2\omega L_{\mathrm{s}} Q(k)}{U_{\mathrm{sm}}(k)} \\ u_{\mathrm{abq}}(k) = \dfrac{2L_{\mathrm{s}}}{U_{\mathrm{sm}}(k)T_{\mathrm{s}}}\left[Q^{*} - Q(k)\right] - \dfrac{2\omega L_{\mathrm{s}} P(k)}{U_{\mathrm{sm}}(k)} \end{cases} \tag{15}$$

where the weighting factor λ is eliminated during the procedure of solving (14). Also the expression and limitation of $u_{\mathrm{ab}\alpha}$ in MP-DPC can be deduced, which is the same as (10) and (11) in DP-DPC.

IV. Relationship between DP-DPC and MP-DPC

A. Inherent relationship of continuous-control-set MP-DPC schemes

Due to those excellent characteristics, several continuous-control-set MP-DPC schemes, from different ways of implementation, have been proposed to improve the control performance of the adopted converter, such as modulation function optimization or duty cycle optimization. Although these schemes are realized in different ways, which adopt the same cost function and mathematical model, the ultimate essence is the same. Taking the MP-DPC with modulation function optimization as an example, the detail analysis is shown as follow.

According to (10) and (15), the expression of $u_{\mathrm{ab}\alpha}$ can be written as

$$\begin{aligned} u_{\mathrm{ab}\alpha}(k) = {} & U_{\mathrm{sm}}(k)\cos\omega t - \frac{2L_{\mathrm{s}}}{U_{\mathrm{sm}}(k)T_{\mathrm{s}}}\left[P^{*} - P(k)\right]\cos\omega t \\ & - \frac{2L_{\mathrm{s}}}{U_{\mathrm{sm}}(k)T_{\mathrm{s}}}\left[Q^{*} - Q(k)\right]\sin\omega t \\ & + \frac{2\omega L_{\mathrm{s}}}{U_{\mathrm{sm}}(k)}\left[P(k)\sin\omega t - Q(k)\cos\omega t\right] \end{aligned} \tag{16}$$

On the basis of (3), the fundamental component expressions of the main voltage u_{s} in α-β reference frame can be defined as

$$\begin{cases} u_{\mathrm{s}\alpha} = U_{\mathrm{sm}}\cos\omega t \\ u_{\mathrm{s}\beta} = U_{\mathrm{sm}}\sin\omega t \end{cases} \tag{17}$$

Then substituting (17) into (16), the expression of modulation index m can be expressed as

$$m(k)=\frac{u_{\mathrm{ab}\alpha}(k)}{u_{\mathrm{dc}}(k)}=\{2\omega L_{\mathrm{s}}T_{\mathrm{s}}\left(P(k)u_{\mathrm{s}\beta}(k)-Q(k)u_{\mathrm{s}\alpha}(k)\right)$$
$$-2L_{\mathrm{s}}u_{\mathrm{s}\alpha}(k)\left(P^{*}-P(k)\right)-2L_{\mathrm{s}}u_{\mathrm{s}\beta}(k)\left(Q^{*}-Q(k)\right) \quad (18)$$
$$+u_{\mathrm{s}\alpha}(k)U_{\mathrm{sm}}^{2}(k)T_{\mathrm{s}}\}/u_{\mathrm{dc}}(k)U_{\mathrm{sm}}^{2}(k)T_{\mathrm{s}}$$

From (18), the expression of m is the same with that of the MP-DPC with modulation function optimization scheme in [8]. Thus, it can be concluded that the inherent character of MP-DPC with modulation function optimization is accordant with that of the conventional MP-DPC. Similarly, the same conclusion also can be obtained between MP-DPC with duty cycle optimization and the conventional MP-DPC. So the internal essence of these continuous- control-set MP-DPC schemes with same cost function and mathematical model are in accordance.

B. Relationship between DP-DPC and continuous-control-set MP-DPC schemes

From (9) and (15), expressions of the control variables $u_{\mathrm{abd}}(k)$ and $u_{\mathrm{abq}}(k)$ in DP-DPC and MP-DPC schemes are the same. In DP-DPC, in order to eliminate the power errors, $P(k+1)$ and $Q(k+1)$ are defined as their reference values P^{*} and Q^{*}. With this definition, (12) will reach the minimized value as zero, which is the main control object of MP-DPC. It is more intuitive that $J(k)$ equals zero while substituting $u_{\mathrm{abd}}(k)$ and $u_{\mathrm{abq}}(k)$ of (9) into (13).

And in MP-DPC, the purpose of calculating the partial derivatives of $u_{\mathrm{abd}}(k)$ and $u_{\mathrm{abq}}(k)$ to $J(k)$ in (14) is to select the appropriate $u_{\mathrm{abd}}(k)$ and $u_{\mathrm{abq}}(k)$ which will predict $P(k+1)$ and $Q(k+1)$ to track their reference values without errors, which is the key definition in DP-DPC. (14) always has a global solution, or a set of $u_{\mathrm{abd}}(k)$ and $u_{\mathrm{abq}}(k)$ always exists that adjusts $J(k)$ to reach the extreme point. Although the powers $P(k+1)$ and $Q(k+1)$ predicted by the optimal $u_{\mathrm{abd}}(k)$ and $u_{\mathrm{abq}}(k)$ may not reach their references during one control interval, the prediction trend of powers is correct, and these predicted powers will reach their own reference values in several control intervals.

According to the above analysis, the essence of DP-DPC and continuous- control-set MP-DPC scheme is similar while the kind of implementation is different.

V. CONTROL PERFORMANCE OBSERVED FROM CIRCUIT EXPERIMENT

A scale-down single-phase PWM converter experimental platform has been implemented to verify the effectiveness of DP-DPC and continuous-control-set MP-DPC schemes. Fig. 4 shows a photo of the experimental hardware prototype platform, which is consist of the main power circuit, signal processing circuit, TMS320F2812 controller and gate signal driving circuit and so on.

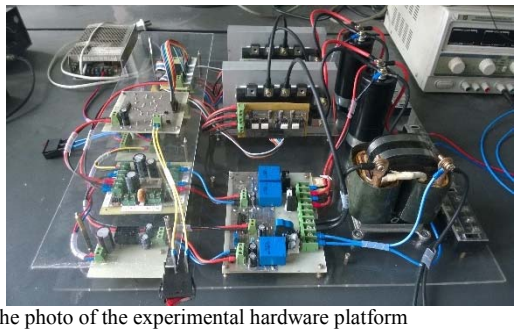

Fig. 4 The photo of the experimental hardware platform

TABLE I
THE PARAMETERS OF EXPERIMENTAL SYSTEM

Parameters	Value
The main voltage(*rms*)U_s/V	60
The dc-link reference voltage U_{dc}^{*}/V	120
The dc-link rated load R_{L}/Ω	30
The ac-side inductor L_s/mH	4.76
The dc-link capacitor C_d/mF	1.65

Due to the same character of these DPC schemes, it just needs to verify the effectiveness of one scheme in those DPC schemes. Table I shows the experimental system parameters, and switching frequency f_s is set as 5kHz.

Fig. 5 *a* shows steady-state experimental waveforms of the main voltage u_s, line current i_s and dc-link voltage u_{dc} of MP-DPC scheme. Fig. 5 *b* shows the FFT analysis results of i_s in MP-DPC scheme in experimental test. Fig. 5 *c* shows experimental waveforms for dynamic response test when the reference active power steps up from 75% to 100% rating value. From Fig. 5, it can be noticed that MP-DPC scheme can achieve perfect steady-state and fast dynamic performance.

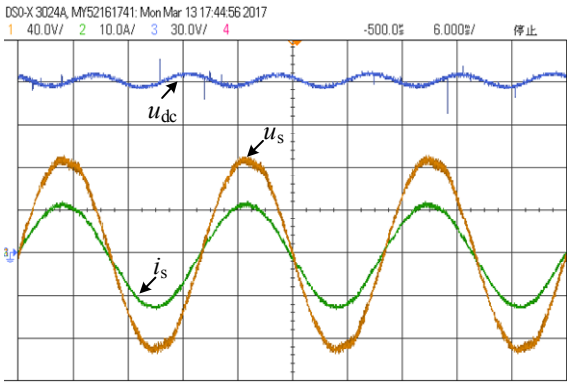

a

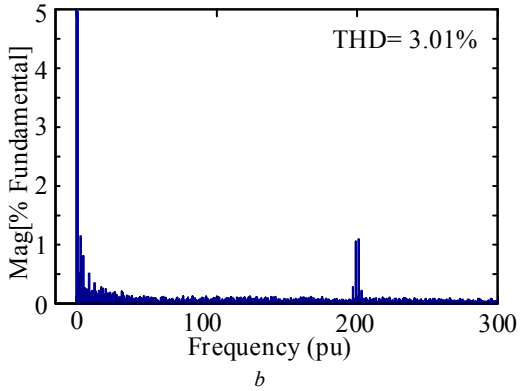

b

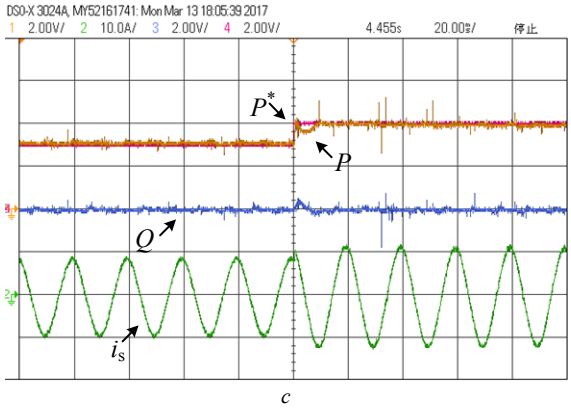

c

Fig. 5 Experimental results of MP-DPC scheme

a Waveforms of the main voltage, line current and dc-link voltage in steady-state (u_s: 40V/div, i_s: 10A/div, u_{dc}:30V/div, Time: 6ms/div)

b FFT analysis result of the line current

c Waveforms of the instantaneous powers while the active reference power steps up from 75% to 100% rating value (P, Q and P^*: 240W/div, i_s: 10A/div, Time: 20ms/div)

VI. Conclusion

This paper presents two kinds of DPC scheme for single-phase PWM converters, which are DP-DPC and conventional continuous-control-set MP-DPC schemes, and verifies their inherent similar relationship. Also, the inner characters of different continuous-control-set MP-DPC schemes with the same cost function and mathematical model are in accordance, such as MP-DPC with modulation function optimization or duty cycle optimization.

Although the design concepts of these schemes are absolutely different, both have the same expressions of reference voltages $u_{abd}(k)$ and $u_{abq}(k)$. The experimental results confirm the good performance of the MP-DPC scheme. Furthermore, this conclusion also applies equally to the direct current control (DCC), that is, deadbeat predictive DCC and continuous-control-set model predictive DCC schemes with PWM stage have the same inherent characteristic.

Acknowledgment

This work was supported in part by the National key R & D program of China under grants 2017YFB1200901.

References

[1] W. Song, S. Wang, C. Xiong, et al, " Single phase three-level SVPWM algorithm for grid-side railway traction converter and its relationship of carrier-based PWM," *IET Electrical Systems in Transportation*, vol.4, no. 3, pp. 78–87, 2014.

[2] J. Norniella, J. Cano, G. Orcajo, et al, " Improving the dynamics of virtual-flux-based control of three-phase active rectifiers", *IEEE Trans. on Industrial Electronics*, vol. 61, no.1, pp. 177-187, Jan. 2014.

[3] Chen, S. and Joos, G., "Direct power control of active filters with averaged switching frequency regulation," *IEEE Trans. on Power Electronics*, vol. 23, no. 10, pp. 2729-2737, 2008.

[4] M. Malinowski, M. Jasinski, and M. Kazmierkowski, "Simple direct power control of three-phase PWM rectifier using space-vector modulation (DPC-SVM)," *IEEE Trans. on Industrial Electronics*, vol. 51, no.2, pp. 447-454, 2004.

[5] W. Song, J. Ma, L. Zhou, et al, "Deadbeat predictive power control of single-phase three-level neutral-point-clamped converters using space-vector modulation for electric railway traction," *IEEE Trans. on Power Electronics*, vol. 31, no. 1, pp. 721–732, 2016.

[6] M. Monfared, M. Sanatkar, and S. Golestan, "Direct active and reactive power control of single-phase grid-tie converters," *IET Power Electronics*, vol.5, no. 8, pp. 1544-1550, 2012.

[7] H. Eskandari-Torbati and D. Khaburi, "Direct power control of three phase PWM rectifier using model predictive control and SVM switching," *Drive Syst. and Technol. Conf. on Power Electronics*, *Iran*, pp. 193-198, April 2013.

[8] W. Song, Z. Deng, S. Wang, et al, "A simple model predictive power control strategy for single-phase PWM converters with modulation function optimization," *IEEE Trans. on Power Electronics*, vol. 31, no. 7, pp. 5279–5289, 2016.

[9] Y. Zhang, W. Xie, Z. Li, et al, "Model predictive direct power control of a PWM rectifier with duty cycle optimization," *IEEE Trans. On Power Electronic*s, vol. 28, no. 11, pp. 5343-5351, 2013.

[10] J. Ma, W. Song, S. Jiao, et al, "Power calculation for direct power control of single-phase three-level rectifiers without phase-locked loop," *IEEE Trans. on Industrial Electronics*, vol.36, no.5, pp. 2871-2882, 2016.

[11] A. Kulkarni and V. John, "A novel design method for SOGI-PLL for minimum settling time and low unit vector distortion," *Proc. IEEE Ind. Electron. Soc. Conf.*, *Vienna*, pp. 274-279, Nov. 2013.